Journal of Molecular Structure 1061 (2014) 61–68

Contents lists available at ScienceDirect

Journal of Molecular Structure

journal homepage: www.elsevier.com/locate/molstruc

Synthesis, characterization and phytotoxic activity of hydroxylated isobenzofuran-1(*3H*)-ones

R.R. Teixeira [a,*], J.L. Pereira [a], S.F. Da Silva [a], S. Guilardi [b,*], D.A. Paixão [b], C.P.A. Anconi [c], W.B. De Almeida [d], J. Ellena [e], G. Forlani [f]

[a] Departmento de Química, Universidade Federal de Viçosa, Viçosa, Minas Gerais, Brazil
[b] Instituto de Química, Universidade Federal de Uberlândia, Uberlândia, Minas Gerais, Brazil
[c] Departamento de Química, Universidade Federal de Lavras, Lavras, Minas Gerais, Brazil
[d] Departamento de Química, Instituto de Ciências Exatas, Universidade Federal de Minas Gerais, Belo Horizonte, Minas Gerais, Brazil
[e] Instituto de Física de São Carlos, Universidade de São Paulo, São Carlos, SP, Brazil
[f] Department of Life Science and Biotechnology, University of Ferrara, Ferrara, Italy

HIGHLIGHTS

- Compounds **3** and **4** crystallized in the space group Pc and $P2_1/n$, respectively.
- DFT calculations confirmed undoubtedly their NMR chemical shifts.
- A good agreement was also obtained for B3LYP/6-31G(d,p) theoretical and experimental IR spectra.
- Isobenzofuran-1(*3H*)-ones **3** and **4** interfere with the radicle growth of monocotyledonous and dicotyledonous species.

GRAPHICAL ABSTRACT

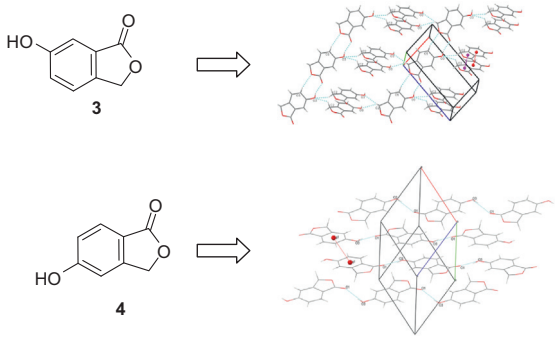

ARTICLE INFO

Article history:
Received 17 September 2013
Received in revised form 17 December 2013
Accepted 18 December 2013
Available online 2 January 2014

Keywords:
Isobenzofuran-1(*3H*)-ones
Phthalides
X-ray analysis
DFT calculations
Phytotoxicity

ABSTRACT

Two hydroxylated isobenzofuranones **3** and **4** were synthesized from benzoic acids. The compounds were fully characterized by IR, NMR (^1H and ^{13}C), HRMS, and X-ray crystallography. Compounds **3** and **4** crystallized in the space group Pc and $P2_1/n$, respectively. DFT calculations were used to confirm undoubtedly their NMR chemical shifts. Biological assays showed that these compounds are capable of interfering with the radicle growth of monocotyledonous and dicotyledonous species, whereas the photosynthetic electron transport chain was substantially unaffected.

1. Introduction

Several natural and synthetic compounds possess a γ-butirolactone fused to a benzene ring. These substances, known as isobenzofuran-1(*3H*)-ones (phthalides), have attracted attention of various research groups due to their wide range of medicinal

* Corresponding authors. Tel.: +55 31 3899 3209/34 3239 4444; fax: +55 31 3899 3065/34 3239 4208.
E-mail addresses: robsonr.teixeira@ufv.br (R.R. Teixeira), silvana@ufu.br (S. Guilardi).

0022-2860/$ - see front matter © 2013 Elsevier B.V. All rights reserved.
http://dx.doi.org/10.1016/j.molstruc.2013.12.059

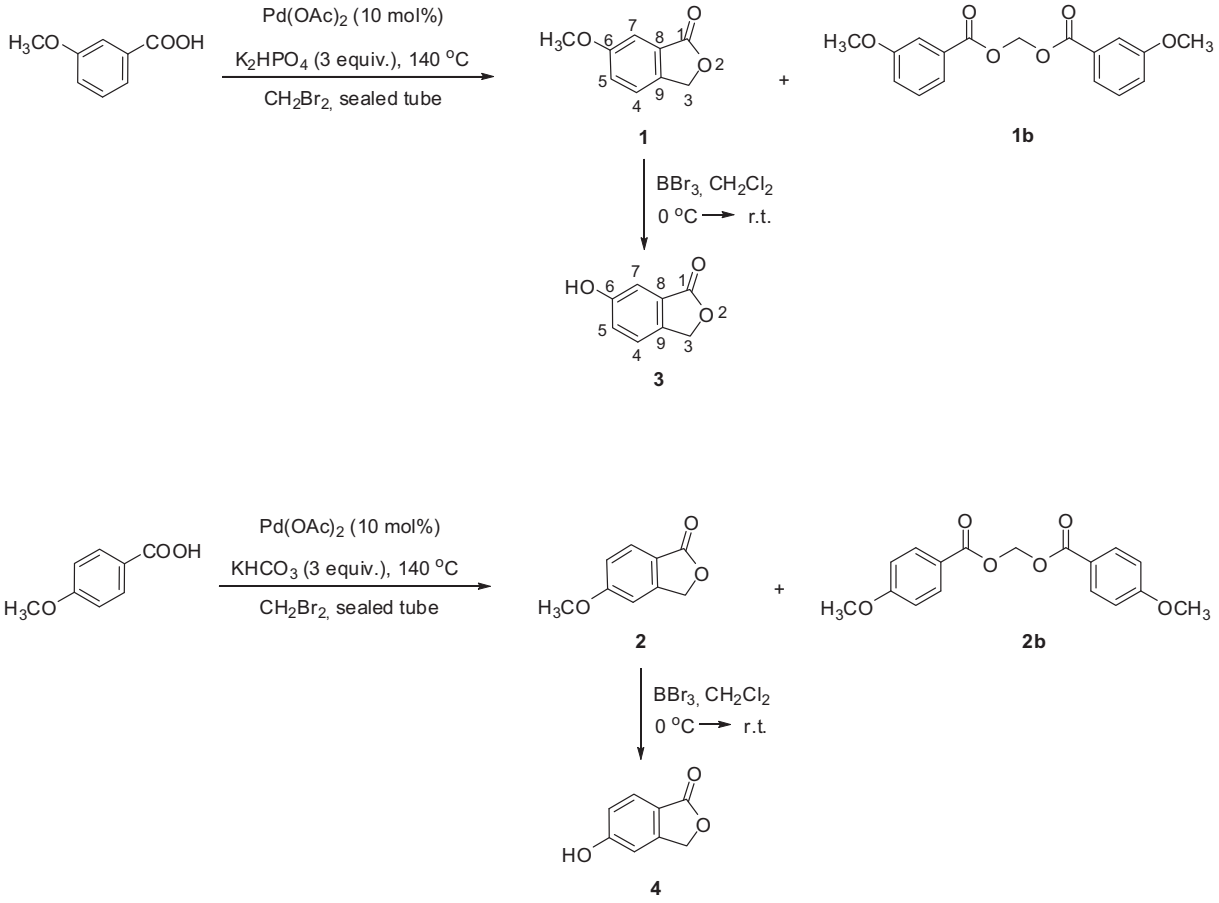

Fig. 1. Synthesis of hydroxylated isobenzofuranones **3** and **4**.

Table 1
Experimental and theoretical (B3LYP/6-311+G(2d,p) ^{13}C NMR and ^{1}H NMR chemical shifts (in ppm), evaluated with respect to TMS, for 6-hydroxyisobenzofuran-1(*3H*)-one **3** and 5-hydroxyisobenzofuran-1(*3H*)-one **4**. Methanol was used as solvent.

Compound	**3**			**4**		
Carbon	Expt.	Theoretical	Deviation[a] (%)	Expt.	Theoretical	Deviation[a] (%)
^{13}C NMR assignments						
C-1	172.5	176.8	2.5	173.7	178.0	2.4
C-3	70.1	70.2	0.1	71.3	71.3	0.0
C-4	123.3	125.8	2.0	110.9	110.2	0.6
C-5	122.8	123.3	0.4	159.8	169.1	5.8
C-6	158.6	162.4	2.4	123.9	119.8	3.3
C-7	109.7	112.1	2.1	127.7	131.5	3.0
C-8	126.6	130.2	2.9	124.4	121.4	2.4
C-9	138.3	143.8	4.0	139.5	157.8	13.1
^{1}H NMR assignments						
H-3	5.25	5.25	0.0	5.25	5.25	0.0
H-4	7.18	7.55	5.1	6.9	6.97	1.0
H-5	7.15	7.25	1.4	–	–	–
H-6	–	–	–	6.95	7.17	3.2
H-7	7.39	7.44	0.7	7.67	7.90	3.1

[a] Percent deviation between experimental and theoretical values ($|expt - theor|/|expt|) \times 100$.

properties which include antiproliferative [1], anticonvulsant [2], antioxidant [3], antiplatelet [4] and anti-HIV [5] activities, and the ability to inhibit ATP synthesis in the chloroplast [6]. Phthalides are also valuable synthetic intermediates such as in the preparation of phenolic derivatives via Houser annulation [7] and in the synthesis of 4,8-dihydroxyisochromanones [8].

In addition to the study of their biological properties [9,10], we are also interested in elucidating the molecular features of isobenzofuran-1(*3H*)-ones [11,12]. In this view, herein we describe the results of a structural investigation of hydroxylated phthalides employing a combination of NMR analyses, XRD techniques and DFT calculations. Their phytotoxic activities were also assessed.

2. Experimental

2.1. Synthesis

2.1.1. Materials and methods

Commercially available 3-methoxy benzoic acid, 4-methoxy benzoic acid, palladium(II) acetate, dibromomethane, potassium dihydrogen phosphate, potassium bicarbonate, boron tribromide 1.0 mol L^{-1} solution in dichloromethane were purchased from Sigma–Aldrich and utilized without further purification. Dichloromethane was purified as described in Perrin and Armarego [13]. Infrared spectra were recorded on a Varian 660-IR, equipped with GladiATR scanning from 4000 to 500 cm^{-1}. HRMS data were recorded under ESI conditions on a micrOTOF—QII Bruker spectrometer. Melting points are uncorrected and were obtained with a MQAPF-301 melting point apparatus (Microquimica, Campinas, Brazil). Analytical thin layer chromatography was carried out on TLC plates recovered with 60GF254 silica gel. Column chromatography was performed over silica gel (60–230 mesh).

2.1.2. Synthesis of 6-methoxy isobenzofuran-1(3H)-one **1**

A tube of 40 mL equipped with a magnetic stir bar was charged with palladium (II) acetate (156.8 mg, 0.70 mmol), potassium dihydrogen phosphate (3654 mg, 21.0 mmol), 3-methoxy benzoic acid (1064 mg, 7.00 mmol) and dibromomethane (28 mL). The tube was sealed with a Teflon cap and the reaction mixture was stirred at 140 °C for 36 h. After this time, the mixture was filtered through a pad of Celite. The filtrate was concentrated under reduced pressure and the residue was purified by silica gel column chromatography (hexane–ethyl acetate 2:1 v/v) to afford the title compound in 59% yield (681 mg, 4.15 mmol) as a white solid. M.p. 116.9–118.4 °C. IR (selected bands, cm^{-1}): 3003, 2925, 2837, 1733, 1600, 1585, 1488, 1454, 1431, 1267, 1206, 1028, 973, 869, 749, 690, 545. ^{1}H NMR (300 MHz, MeOH-d_4) δ: 3.87 (s, 3H, —OC<u>H</u>$_3$), 5.26 (s, 2H, H-3), 7.22–7.38 (m, 3H, H-4, H-5 and H-7); ^{13}C NMR (75 MHz, MeOH-d_4) δ: 56.0 (—O<u>C</u>H$_3$), 69.7 (C-3), 107.7 (C-7), 123.1 (C-5), 123.3 (C-4), 127.3 (C-8), 139.1 (C-9), 160.8 (C-6), 171.4 (C-1). HREIMS m/z (M+H+): Calcd for $C_9H_8O_3$, 165.0552; found: 165.0608.

2.1.3. Synthesis of 5-methoxy isobenzofuran-1(3H)-one **2**

A tube of 40 mL equipped with a magnetic stir bar was charged with palladium(II) acetate (67.3 mg, 0.30 mmol), potassium bicarbonate (750 mg, 7.50 mmol), 4-methoxybenzoic acid (456 mg, 3.00 mmol) and dibromomethane (12 mL). The tube was sealed with a Teflon cap and the reaction mixture was stirred at 140 °C for 18 h. After this time, the mixture was filtered through a pad of Celite. The filtrate was concentrated under reduced pressure and the residue was purified by silica gel column chromatography eluted with hexane–ethyl acetate (2:1 v/v) to afford 5-methoxyisobenzofuran-1(*3H*)-one **2** in 33% yield (164 mg, 1.00 mmol). M.p. 113.4–114.7 °C. IR (selected bands, cm^{-1}): 3032, 2922, 2852, 1736, 1601, 1489, 1452, 1361, 1333, 1261, 1146, 1036, 986, 773. ^{1}H NMR (300 MHz, $CDCl_3$) δ: 3.89 (s, 3H, —OC<u>H</u>$_3$), 5.25 (s, 2H,

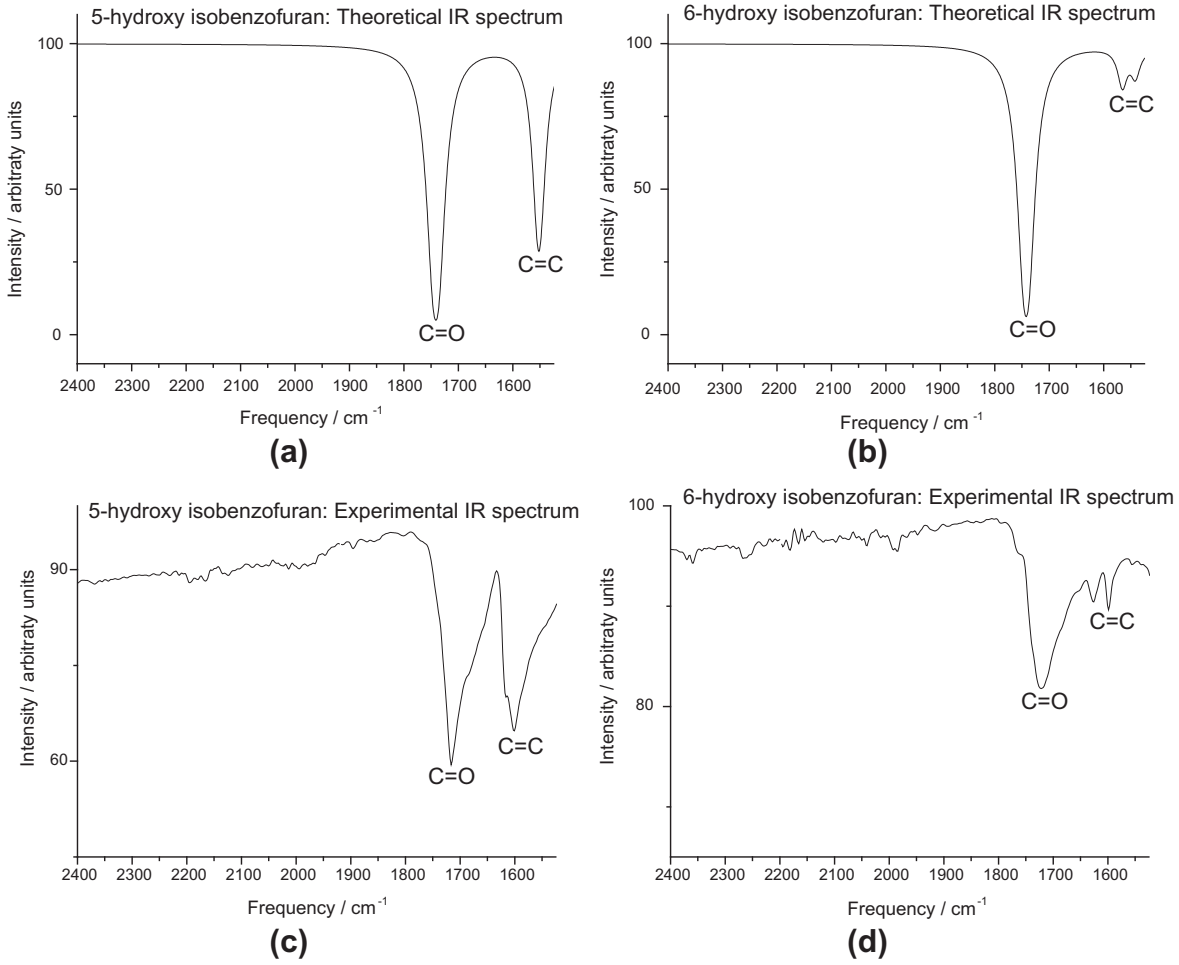

Fig. 2. B3LYP/6-31G(d,p) theoretical (a and b) and experimental (c and d) IR spectra for compounds **3** and **4**.

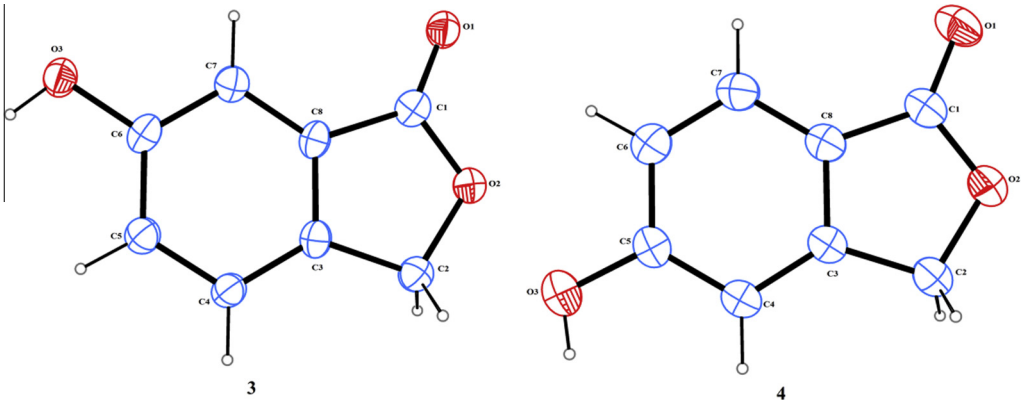

Fig. 3. ORTEP drawings of compounds **3** and **4** with the atom numbering scheme. Displacement ellipsoids for non-H atoms were drawn at the 30% probability level.

Table 2
Crystallographic data and details of diffraction experiments for the compounds **3** and **4**.

Compound	**3**	**4**
Empirical formula	$C_8H_6O_3$	$C_8H_6O_3$
Formula weight (g mol^{-1})	150.13	150.13
Temperature (K)	100(2)	293(2)
Crystal system	Monoclinic	Monoclinic
Space group	Pc	$P2_1/n$
Unit cell dimensions (Å,°)		
a	7.066(6)	7.6506(15)
b	3.880(3)	12.349(4)
c	12.445(11)	7.8409(11)
β	105.85(5)	117.453(10)
Volume (Å^3), *Z*	328.2(5), 2	657.3(2), 4
Calculated density (g cm^{-3})	1.519	1.517
Absorption coefficient (mm^{-1})	0.996	0.118
F(000)	156	312
Crystal size (mm)	0.28 × 0.16 × 0.11	0.24 × 0.11 × 0.07
2*θ* range for data collection (°)	6.51–63.14	3.08–27.47
Limiting indices	−7, 8; −4.4; −12, 11	−9.9; −15.15; −10.9
Reflections collected/unique	1111/754 [*R*(int) = 0.0346]	5950/1461 [*R*(int) = 0.0338]
Goodness-of-fit on F^2	1.171	1.039
Data/restraints/parameters	754/2/100	1461/0/100
Final *R* indices [$I > 2\sigma(I)$]	*R* = 0.0451, *wR* = 0.1160	*R* = 0.0533, *wR* = 0.1430
R indices (all data)	*R* = 0.0457, *wR* = 0.1199	*R* = 0.0807, *wR* = 0.1633
Largest difference peak and hole (e A^{-3})	0.198 and −0.200	0.198 and −0.193

$R = \Sigma(||F_o| - |F_c||)/\Sigma|F_o|; wR = [\Sigma w(|F_o^2| - |F_c^2|)^2/\Sigma w|F_o^2|^2]^{1/2}$.

H-3), 6.91 (d, 1H, *J* = 0.6 Hz, H-4), 7.02 (dd, 1H, *J* = 8.4, 0.6 Hz, H-6), 7.80 (d, 1H, *J* = 8.4 Hz, H-7). ^{13}C NMR (75 MHz, $CDCl_3$) *δ* 56.1 (—O<u>C</u>H$_3$), 69.3 (C-3), 106.2 (C-4), 116.7 (C-6), 118.2 (C-8), 127.4 (C-7), 149.6 (C-9), 164.9 (C-5), 171.1 (C-1). HREIMS m/z (M+H+): Calcd for $C_9H_8O_3$, 165.0552; found: 165.0606.

2.1.4. Synthesis of 6-hydroxy isobenzofuran-1(3H)-one **3**

A 25 mL two necked round bottom flask, under nitrogen atmosphere, was charged with 6-methoxy isobenzofuran-1(*3H*)-one **1** (100 mg, 0.61 mmol) and anhydrous dichloromethane (5 mL). The resulting mixture was magnetically stirred and cooled in ice bath for 10 min. After that, 1.8 mL of 1.0 mol L^{-1} BBr_3 solution in dichloromethane (1.8 mmol) was added dropwise. Then, the reaction mixture under continuous magnetic stirring was allowed to warm up to room temperature. Subsequently, 5 mL of distilled water were added and the mixture was transferred to a separatory funnel and extracted with ethyl acetate (3 × 25 mL). The combined organic extracts were dried over magnesium sulphate, filtrated and concentrated under reduced pressure. The residue was purified by column chromatography eluted with hexane–ethyl acetate (2:1 v/v) to afford compound **3** as yellow solid in 92% yield (84 mg, 0.56 mmol). Suitable crystals for XRD analysis were obtained by slow crystallization from water. M.p. 198.6–201.3 °C. IR (selected bands, cm^{-1}): 3252 (broad band), 2959, 2922, 2851, 1726, 1623, 1599, 1491, 1447, 1366, 1312, 1052, 990, 771, 542 cm^{-1}. ^{1}H NMR (300 MHz, MeOH-d_4) *δ*: 5.25 (s, 2H, H-3), 7.15–7.18 (m, 2H, H-5 and H-4), 7.39 (d, 1H, *J* = 9.0 Hz, H-7). ^{13}C NMR (75 MHz, MeOH-d_4) *δ*: 70.1 (C-3), 109.7 (C-7), 122.8 (C-5), 123.3 (C-4), 126.6 (C-8), 138.3 (C-9), 158.6 (C-6), 172.5 (C-1). HREIMS m/z (M+H+): Calculated for $C_8H_7O_3$, 151.0395; found: 151.0370.

2.1.5. Synthesis of 5-hydroxy isobenzofuran-1(3H)-one **4**

Compound **4** was synthesized in 83% yield using a similar procedure to that described for compound **3**. Structure of phtalide **4** is supported by the data described below. Suitable crystals for XRD analysis were obtained by slow crystallization from acetone. Pale yellow solid. M.p. 226.8–227.3 °C. IR (selected bands, cm^{-1}): 3261 (broad band), 2925, 2855, 1714, 1597, 1432, 1340, 1275, 1057, 1007, 937 cm^{-1}. ^{1}H NMR (300 MHz, MeOH-d_4) *δ*: 5.25 (s, 2H; H-3), 6.95–6.90 (m, 2H; H-6 and H-4); 7.67 (d, *J* = 9.0 Hz, 1H, H-7). ^{13}C NMR (75 MHz, MeOH-d_4) *δ*: 71.3 (C-3), 110.9 (C-4), 123.9 (C-6), 124.4 (C-8), 127.7 (C-7), 139.5 (C-9), 159.8 (C-5),

173.7 (C-1). HREIMS m/z (M+H+): Calculated for $C_8H_7O_3$, 151.0395; found: 151.0369.

2.2. X-ray Crystallography

A white crystal with approximate dimensions of 0.28 × 0.16 × 0.11 mm of the compound **3** was selected for data collection. The X-ray diffraction data were collected on a Bruker APEX II diffractometer equipped with a CCD area detector and a graphite monochromator utilizing Cu Kα radiation (λ = 1.54178 Å) at 100(2) K. Data collection, cell refinement and data reduction were made using APEX2 software [14]. Final unit cell parameters based on all reflections were obtained by least squares refinement. The data were integrated via SAINT [15]. Lorentz and polarization effect and multi-scan absorption corrections were applied with SADABS [16]. The integration of the data using a monoclinic unit cell yielded a total of 1111 reflections to a maximum θ angle of 63.14° (0.86 Å resolution), of which 754 were independent (average redundancy 1.473, completeness = 79.5%, Rint = 3.46%) and 738 (97.88%) were greater than $2\sigma(F^2)$.

A yellow crystal with approximate dimensions of 0.24 × 0.11 × 0.07 mm of the compound **4** was selected for data collection. Intensity data collections were carried out on an Enraf–Nonius Kappa-CCD diffractometer using a graphite monochromator with Mo Kα radiation (0.71073 Å), at room temperature. Data collections were made using the COLLECT program [17]. The final unit cell parameters were based on all reflections; integration and scaling of the reflections, correction for Lorentz and polarization effects were performed with the DENZO-SMN system of programs [18]. The data set consisted a total of 5950 reflections, of which 1461 were independent (Rint = 3.38%) and 984 were greater than $2\sigma(F^2)$.

The structures were solved by direct methods with SHELXS-97 [19]. The models were refined by full-matrix least-squares on F^2 with SHELXL-97 [19]. Hydrogen atoms in their calculated positions were refined using a riding model. The non-hydrogen atoms were refined anisotropically. Structural representations were drawn using ORTEP-3 [20] and MERCURY [21]. The program WinGX [22] was used to prepare materials for publication. Data collections and experimental details for **3** and **4** are summarized in Table 2.

2.3. DFT calculations

Density Functional Theory (DFT) [23] calculations using the B3LYP functional [24,25] and the 6-31G(d,p) and 6-311+G(2d,p) basis sets [26,27] (named B3LYP/6-31G(d,p) and B3LYP/6-311+G(2d,p) levels) were carried out for geometry optimization and also harmonic frequency calculations which yield directly the infrared (IR) spectrum. The crystallographic structures (X-ray coordinates) were used as starting point for B3LYP geometry optimization procedures. The gauge-independent atomic orbital (GIAO) method implemented by Wolinski, Hilton and Pulay [28] was used for DFT calculations of ^{1}H and ^{13}C magnetic shielding constants (σ), with chemical shifts (δ), obtained on a δ-scale relative to the TMS, taken as reference. The solvent effect (methanol: ε = 32.7) was accounted for using the polarizable continuum model (PCM) by the integral equation formalism (IEFPCM) [29], in single point NMR calculations on the fully optimized geometries in the vacuum. Such theoretical procedure that enables undoubtedly the identification of NMR chemical shifts of the isobenzofuranones **3** and **4** was previously used successfully in conformational analysis [30,31]. In addition to NMR spectra, the calculated theoretical IR spectra were used for comparison with experimental spectroscopic data at the B3LYP/6-31G(d) level of theory. All calculations were carried out with the Gaussian-03 program [32] and the theoretical spectra have been obtained according to Dos Santos and co-workers' procedure [33].

Table 3
Bond lengths (Å) and angles (°) for compounds **3** and **4**.

Compound	3		4	
	Expt.	Theor.	Expt.	Theor.
Bond lengths				
O(2)—C(1)	1.350(4)	1.37	1.354(2)	1.38
O(2)—C(2)	1.463(5)	1.44	1.453(2)	1.44
O(1)—C(1)	1.211(5)	1.20	1.219(2)	1.20
C(1)—C(8)	1.464(5)	1.48	1.453(2)	1.47
C(8)—C(3)	1.379(5)	1.39	1.380(2)	1.38
C(8)—C(7)	1.387(4)	1.39	1.381(3)	1.39
C(7)—C(6)	1.387(5)	1.39	1.378(2)	1.38
C(6)—C(5)	1.397(6)	1.40	1.393(3)	1.40
C(5)—C(4)	1.404(5)	1.39	1.394(3)	1.40
C(4)—C(3)	1.394(5)	1.39	1.379(2)	1.39
C(3)—C(2)	1.496(5)	1.50	1.493(3)	1.50
O(3)—C(6)	1.371(4)	1.37	–	
O(3)—C(5)	–		1.357(2)	1.36
Bond angles				
C(1)—O(2)—C(2)	111.2(3)	111	110.06(14)	111
O(1)—C(1)—O(2)	121.3(3)	123	119.72(17)	122
O(1)—C(1)—C(8)	129.9(3)	130	131.21(18)	131
O(2)—C(1)—C(8)	108.7(3)	107	109.06(14)	107
C(3)—C(8)—C(7)	123.7(3)	123	121.26(15)	121
C(3)—C(8)—C(1)	107.6(3)	109	108.27(16)	109
C(7)—C(8)—C(1)	128.6(3)	129	130.47(15)	130
C(8)—C(7)—C(6)	116.6(3)	117	118.16(15)	118
C(7)—C(6)—C(5)	120.9(4)	121	120.72(17)	120
C(6)—C(5)—C(4)	121.6(3)	121	120.98(15)	121
C(3)—C(4)—C(5)	117.3(3)	118	117.54(16)	118
C(8)—C(3)—C(4)	119.9(3)	120	121.34(17)	121
C(8)—C(3)—C(2)	109.5(3)	108	108.14(15)	108
C(4)—C(3)—C(2)	130.6(3)	132	130.51(16)	131
O(2)—C(2)—C(3)	103.0(3)	105	104.44(14)	105
O(3)—C(6)—C(7)	116.7(3)	117	–	
O(3)—C(6)—C(5)	122.4(3)	122	–	
O(3)—C(5)—C(6)	–		116.44(17)	117
O(3)—C(5)—C(4)	–		122.58(16)	122

2.4. Radicle elongation assay on filter paper

Bioassays were carried out using Petri dishes (90 mm diameter) with one sheet of Whatman No. 1 filter paper as substrate. Germination and growth were conducted in aqueous solutions at controlled pH by using 0.02 mol L^{-1} [*N*-morpholino]ethanesulfonic acid (MES) buffer, brought to pH 6.0 with NaOH 1.0 mol L^{-1}. Compounds to be assayed were dissolved in dimethyl sulfoxide (DMSO) at different concentrations and these solutions were diluted with buffer (0.5% v/v of DMSO) so that test concentrations for the compound (10^{-3} and 10^{-5} mol L^{-1}) were reached. This procedure facilitated the solubility of the compounds. Twenty seeds of each target species (*Allium cepa* and *Cucumis sativus*) were placed in each Petri dish. Treatments and negative controls (buffered aqueous solutions with DMSO and without any tested compound) were added (5 mL) to each Petri dish. Petri dishes were sealed with Parafilm to ensure closed-system models. Seeds were further incubated at 25 °C in a controlled-environment growth chamber, in the absence

Table 4
Hydrogen bonds for compounds **3** and **4**.

Donor—H···Acceptor	d(D—H)	d(H···A)	d(D···A)	<(DHA)
*Compound **3***				
O(3)—H···O(1)^{i}	0.84	1.91	2.699(4)	155.8
C(5)—H(5)···O(2)^{i}	0.95	2.53	3.450(5)	163.7
C(2)—H(2B)···O(3)^{ii}	0.99	2.53	3.430(5)	151.7
C(2)—H(2A)···O(3)^{iii}	0.99	2.56	3.255(5)	127.2
*Compound **4***				
O(3)—H···O(1)^{iv}	0.82	1.93	2.735(2)	167.1

Symmetry codes: (i) $x+1$, $y+1$, z; (ii) $x-1$, $-y+2$, $z-1/2$; (iii) $x-1$, $-y+1$, $z-1/2$; (iv) $x-1$, y, $z-1$.

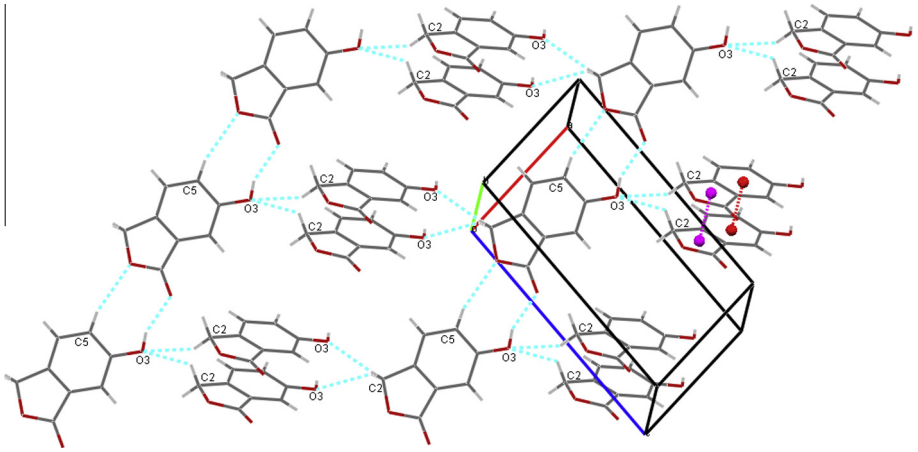

Fig. 4. A portion of the crystal packing of compound **3** viewed approximately down the b axis. Dotted lines denote O—H···O and C—H···O interactions. Centroids of benzene rings are drawn as red balls and lactone rings as pink balls. (For interpretation of the references to colour in this figure legend, the reader is referred to the web version of this article.)

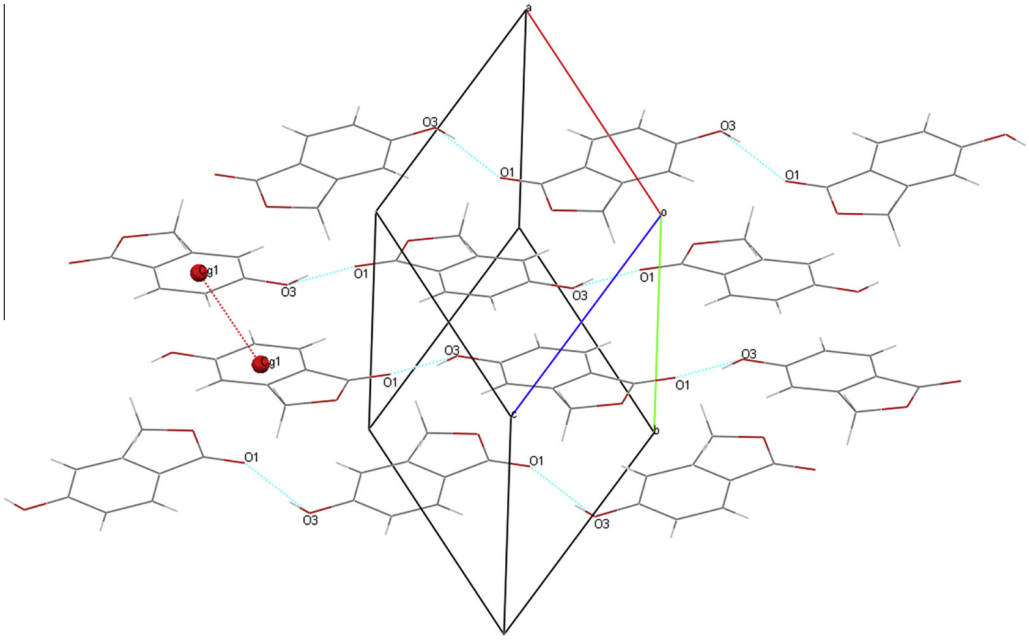

Fig. 5. A packing diagram of compound **4**. The O—H···O and π–π interactions are shown as dotted lines. Centroids of benzene rings are drawn as red balls. (For interpretation of the references to colour in this figure legend, the reader is referred to the web version of this article.)

of light. Bioassays took 7 days. After growth, plants were frozen at −10 °C for 24 h to avoid subsequent growth during the measurement process. This facilitated the handling of the plants and allowed a more accurate measurement of radicle elongation. The radicle length was measured to the nearest millimeter. All treatments were replicated four times in a completely randomized design. The percentage of radicle growth inhibition or stimulation was calculated in relation to the radicle length of the control. *A. cepa* and *C. sativus* seeds (TOPSEED brand) were purchased from Agristar do Brazil, Petrópolis, Rio de Janeiro State, Brazil.

Table 5
Effect of isobenzofuran-1(*3H*)-ones **1**–**4** on radicle growth of *C. sativus* and *A. cepa* seedlings.

Compound	*A. cepa*		*C. sativus*	
	10^{-3} mol L^{-1}	10^{-5} mol L^{-1}	10^{-3} mol L^{-1}	10^{-5} mol L^{-1}
	Inhibition or stimulation (%)		Inhibition or stimulation (%)	
1	−36.3	+2.64	−57.0	−11.7
2	−63.1	−40.0	−37.7	−5.60
3	−23.8	+1.30	−38.9	−3.20
4	−29.1	−10.6	−14.4	+4.62

(−) Means inhibitory effect; (+) means stimulatory effect.

2.5. Measurement of the photosynthetic electron transport

The chloroplastic electron transport chain was measured by following the light-dependent reduction of ferricyanide by isolated thylakoid membranes, as previously described [10,34]. Briefly, deveined plant material was homogenized in 100 mL of ice-cold 20 mM Tricine-NaOH buffer (pH 8.0) containing 10 mM NaCl, 5 mM $MgCl_2$ and 0.4 M sucrose. The homogenate was filtered through surgical gauze and the filtrate was centrifuged at 4 °C for 1 min at 500*g*; the supernatant was further centrifuged for

10 min at 1500*g*. Pelleted chloroplasts were osmotically swollen by resuspension in sucrose-lacking buffer, immediately diluted 1:1 with sucrose-containing buffer, and kept on ice in the dark until used. Aliquots of membrane preparations corresponding to 15 μg chlorophyll were incubated at 24 °C in 1-mL cuvettes containing 20 mM Tricine–NaOH buffer (pH 8.0), 10 mM NaCl, 5 mM $MgCl_2$, 0.2 M sucrose and 1 mM $K_3[Fe(CN)_6]$. The assay was initiated by exposure to saturating light, and the rate of ferricyanide reduction was measured at 1-min intervals for 15 min. Isobenzofuranones were dissolved and diluted in DMSO. Their effect upon the photosynthetic electron transport was evaluated in parallel assays in which 2.5% (v/v) of a suitable dilution was added to the reaction mixture so as to obtain the desired final concentration. Results were expressed as percentage of controls treated with DMSO alone. Reported values are mean ± SE over 4 replicates.

3. Results and discussion

3.1. Synthesis of hydroxylated isobenzofuranones

To synthesize isobenzofuran-1(3*H*)-ones **3** and **4** we started with 3-methoxy benzoic acid and 4-methoxy benzoic acid (Fig. 1). Thus, the palladium(II) catalyzed *ortho* alkylation of these benzoic acids [35] afforded substances **1** and **2** in, respectively, 59% and 33% yields after purification by column chromatography. The diesters **1b** and **2b**, which are formed as a consequence of the nucleophilic substitution between the substrate and dibromomethane, were also isolated. Dimethylation of isobenzofuranones **1** and **2** with BBr_3 [36] gave hydroxylated derivatives **3** (92% yield) and **4** (83% yield).

3.2. DFT calculations

NMR chemical shifts (^{1}H and ^{13}C) were undoubtedly identified through the aid of B3LYP/6-311+G(2d,p) theoretical data for compounds **3** and **4**. Calculated and measured chemical shift data are given in Table 1, along with the deviation between experimental and theoretical NMR results. A very good agreement between theoretical and experimental values was observed for compound **3**, being this compound precisely characterized by the DFT NMR calculations. Data for compout **4** are also very good regarding the ^{1}H NMR spectra, with an average deviation below 5% observed. The ^{13}C NMR chemical shift shows a sizeable deviation only for C-9 carbon atom (13%) with a good agreement found for the other chemical shift values (less than 5% deviation). A similar behavior has also been found in previous work for epoxide quebrachitol derivatives [30], which do not invalidate the use of theoretical ^{13}C NMR data for structural determination.

A good agreement was also obtained for B3LYP/6-31G(d,p) theoretical and experimental IR spectra in the 2400–1500 cm^{-1} region (Fig. 2). These analyses can be very helpful since the IR spectral profile is also affected by changes in the molecular structure and immediate local chemical environment. It can be seen from Fig. 2 that the theoretical IR spectrum for both compounds **3** and **4** reproduces well the experimental spectral profile in the 2000–1500 cm^{-1} finger print region. The noticeable peak around 1600 cm^{-1} (C=C stretching) for compound **4** is correctly reproduced by the theoretical spectrum, as well as the absorption band around 1700 cm^{-1} that corresponds to C=O stretching. The main characteristic of compound **3** is the drastic reduction of intensity of the C=C stretching mode which is precisely reproduced by the theoretical calculations. It should be mentioned that the B3LYP calculated harmonic frequencies were scaled by a factor of 0.93 in order to obtain an agreement with the experimentally observed vibrational frequencies which are not true harmonic oscillators. This procedure was well justified and successfully used in our previous combined experimental and theoretical work [30]. The similarities of the compounds **3** and **4** and the correct identification of the spectral profile reinforce the accuracy of the theoretical prediction at B3LYP level of theory, an aspect that can be explored in the area of organic synthesis mainly in synthetic routes for which more than one product is expected.

3.3. XRD analysis

The atom numbering scheme of compounds **3** and **4** are shown in Fig. 3.

Crystallographic data and details of diffraction experiments are provided in Table 2. Bond distances and angles are given in Table 3. Theoretical structural data are also given in Table 3 showing a good agreement with experiment and so corroborating structure determination. Compound **3** crystallizes in the non-centrosymmetric space group Pc. In the absence of significant anomalous scatters in the molecule, attempts to confirm the absolute structure by refinement of the Flack parameter in the presence of 327 sets of Friedel equivalents led to an inconclusive value of −0.2(4).

In both structures the geometric parameters are within the values expected for this class of compounds [37] and are consistent with the data reported for similar structures [11,12,37–40]. The C2—O2 bond lengths [1.463(2) Å (compound **3**) and 1.453(2) Å (compound **4**)] are consistent with the expected value for a C—O single bond and the C1—O2 bond lengths [1.350(2) Å and 1.354(3) Å, respectively, for compounds **3** and **4**] have double bond character. The C2—C3 bond is larger than C1—C8. Similar behavior is observed for phtalide [41] and methoxylated compounds (**1**) and (**2**) [11,12].

In compounds **3** and **4**, the molecule is essentially planar with root mean-square deviation to the fitted non-hydrogen atoms of 0.018(2) Å and 0.014(2) Å, respectively. The compound without substituents attached to the aromatic ring (phtalide) has a deviation of 0.014 Å [41].

The molecular packing in both structures is mainly determined by intermolecular O3—H···O1 hydrogen bond between the hydroxyl and carbonyl groups (Table 4). In the crystal of compound **3**, this hydrogen bond and a weak C5—H5···O2 interaction assemble the molecules in two-dimensional network along [1 1 0] direction. There are also two C—H···O intermolecular interactions, where the O3 atom acts as a bifurcated acceptor, and π–π stacking between adjacent molecules involving benzene rings [Cg1–Cg1 = 3.88 Å; symmetry code: x, $-1+y$, z] and lactone rings [Cg2–Cg2 = 3.88 Å; symmetry code: (x, $1+y$, z)] forms a three dimensional network (Fig. 4).

Table 6
Effect of isobenzofuranones on light-driven ferricyanide reduction by isolated spinach chloroplasts.

Concentration	10^{-5} mol L^{-1}	3×10^{-5} mol L^{-1}	10^{-4} mol L^{1}	3×10^{-4} mol L^{-1}	10^{-3} mol L^{-1}
Compound					
1	+5.4 (±2.5)	+2.6 (±1.7)	+3.5 (±1.4)	−6.9 (±4.5)	−11.4 (±2.4)
2	+2.0 (±0.6)	+2.3 (±2.8)	−0.3 (±0.6)	−13.3 (±1.9)	−16.4 (±0.2)
3	+3.6 (±1.1)	+1.2 (±1.5)	+1.3 (±2.5)	−10.8 (±3.1)	−23.4 (±1.1)
4	+5.2 (±1.0)	+7.8 (±2.9)	+16.1 (±6.3)	+20.2 (±0.8)	+17.6 (±2.4)

(−) Means inhibitory effect; (+) means stimulatory effect.

In the crystal packing of compound **4**, the hydrogen bond O3—H···O1 links the molecules in a two-dimensional network along [101] direction. The molecules are further connected by π–π interactions between benzene rings of molecules related by an inversion center [Cg1–Cg1 = 3.90 Å; symmetry code: $-x$, $-y$, $-z$] (Table 4 and Fig. 5).

3.4. Biological activity

The isobenzofuranones **3** and **4**, as well as their methoxylated precursors **1** and **2** were evaluated for the ability to interfere with the radicle growth of *C. sativus* (a dicotyledonous species) and *A. cepa* (a monocotyledonous species) at two different concentrations (10^{-3} and 10^{-5} mol L^{-1}) and results are presented in Table 5.

At the higher concentration, compounds **1** and **2** significantly inhibited the radicle growth of both species. The hydroxylated derivatives **3** and **4** also presented inhibitory activity, but less pronounced. At 10^{-5} mol L^{-1} the effects were almost negligible, with the exception of compound **2**, which caused 40.0% inhibition against *A. cepa*. A slight stimulation was on the contrary found for phthalides **1**, **3** and **4**.

The occurrence of a significant growth inhibition in dark-grown seedlings implies that the synthesized phthalides may target some aspect(s) of heterotrophic plant metabolism. However, because some other isobenzofuranones have been previously found to interfere with the photosynthetic process [6,10], their ability of inhibiting *in vitro* the chloroplastic electron transport chain was also investigated. Results, summarized in Table 6, showed that at high concentrations compounds **1**, **2** and **3** are indeed capable of significantly lowering the rate of ferricyanide reduction by thylakoid membranes. This notwithstanding, the effect was remarkably lower than (and unrelated to) that pointed out on radicle growth.

4. Conclusion

In this investigation, we synthesized and fully characterized by IR, NMR and X-ray single crystal diffraction two hydroxylated isobenzofuranones. Calculated chemical shifts and vibrational wavenumbers are in good agreement with experimental data. The phytotoxic evaluation of the hydroxylated isobenzofuranones (and their methoxylated precursors) showed that the compounds are capable of interfering with the radicle growth of monocotyledonous and dicotyledoneous species. Measurements of the Hill reaction suggest that the interference with the photosynthetic electron transport, if any, would play a minor role in their phytotoxicity.

Supplementary material

Crystallographic data for the structures reported in this paper have been deposited with the Cambridge Crystallographic Data Center as supplementary publication. CCDC 960021 (compound **3**) and CCDC 959738 (compound **4**). Copies of the data can be obtained free of charge on application to CCDC, 12 Union Road, Cambridge CB2 1EZ, UK (e-mail: deposit@ccdc.cam.ac.uk).

Acknowledgments

We are grateful to FAPEMIG for financial support. This work is a collaboration research project of Rede Mineira de Química (RQ-MG) also supported by FAPEMIG. We are also grateful to CNPq for research fellowship (to J. Ellena) and Laboratório multiusuário for X-ray diffraction data collection in ApexII Bruker:Facility para Estudos Avançados de Materiais/FAMa (projeto FAPESP No. 2009/54035-4).

References

[1] L.P.L. Logrado, C.O. Santos, L.A.S. Romeiro, A.M. Costa, J.R.O. Ferreira, B.C. Cavalcanti, M.O. De Moraes, L.V. Costa-Lotufo, C. Pessoa, M.L. Dos Santos, Eur. J. Med. Chem. 45 (2010) 3480–3489.
[2] J.A. Cardozo, R. Braz-Filho, J. Rincón-Velandia, M.F. Guerrero-Pabón, Rev. Col. Cienc. Quím. Farm. 34 (2005) 69–76.
[3] X.-Z. Huang, Y. Zhu, X.-L. Guan, K. Tian, J.-M. Guo, H.-B. Wang, G.-M. Fu, Molecules 17 (2012) 4219–4224.
[4] F. Ma, Y. Gao, H. Qiao, X. Hu, J. Chang, J. Thromb. Thrombolysis 33 (2012) 64–73.
[5] K. Yogonathan, C. Rossant, S. Ng, Y. Huang, M.S. Butler, A.D. Buss, J. Nat. Prod. 66 (2003) 1116–1117.
[6] A.J. Demuner, L.C.A. Barbosa, T.A.M. Veiga, R.W. Barreto, B. King-Diaz, B. Lotina-Hennsen, Biochem. Syst. Ecol. 34 (2006) 790–795.
[7] D. Mal, P. Pahari, Chem. Rev. 107 (2007) 1892–1918.
[8] B.A. Egan, M. Paradowski, L.H. Thomas, R. Marquez, Org. Lett. 13 (2011) 2086–2089.
[9] R.R. Teixeira, G.C. Bressan, W.L. Pereira, J.G. Ferreira, F.M. De Oliveira, D.C. Thomaz, Molecules 18 (2013) 1881–1896.
[10] R.R. Teixeira, W.L. Pereira, D.C. Tomaz, F.M. de Oliveira, S. Giberti, G. Forlani, J. Agric. Food Chem. 61 (2013) 5540–5549.
[11] J.L. Pereira, R.R. Teixeira, S. Guilardi, D.A. Paixão, Acta Cryst. E68 (2012) o295.
[12] D.A. Paixao, S. Guilardi, J.L. Pereira, R.R. Teixeira, J.F. Arantes, Acta Cryst. E68 (2012) o3288.
[13] D.D. Perrin, W.L.F. Armarego, Purification of Laboratory Chemicals, third ed., Pergamon, Oxford, 1988.
[14] Bruker, APEX2, Bruker AXS Inc., Madison, Wisconsin, USA, 2004.
[15] Bruker, SAINT, AXS Inc., Madison, Wisconsin, USA, 2007.
[16] Bruker, SADABS, Bruker AXS Inc., Madison, Wisconsin, USA, 2002.
[17] Enraf-Nonius COLLECT, Nonius BV, Delft, The Netherlands, 1997–2000.
[18] Z. Otwinowski, W. Minor, in: C.W. Carter Jr., R.M. Sweet (Eds.), Methods in Enzymology, vol. 276, Academic Press, New York, 1997, p. 307.
[19] G.M. Sheldrick, Acta Cryst. A64 (2008) 112.
[20] L.J. Farrugia, J. Appl. Cryst. 30 (1997) 565.
[21] C.F. Macrae, P.R. Edgington, P. McCabe, E. Pidcock, G.P. Shields, R. Taylor, M. Towler, J. van de Streek, J. Appl. Cryst. 39 (2006) 453.
[22] L.J. Farrugia, J. Appl. Cryst. 32 (1999) 837.
[23] R.G. Parr, W. Yang, Density Functional Theory of Atoms and Molecules, Oxford University Press, Oxford, 1989.
[24] A.D. Becke, J. Chem. Phys. 98 (1993) 5648–5652.
[25] C. Lee, W. Yang, R.G. Parr, Phys. Rev. B 37 (1988) 785–789.
[26] R. Ditchfield, W.J. Hehre, J.A. Pople, J. Chem. Phys. 54 (1971) 724–728.
[27] W.J. Hehre, R. Ditchfield, J.A. Pople, J. Chem. Phys. 56 (1972) 2251–2257.
[28] K. Wolinski, J.F. Hilton, P. Pulay, J. Am. Chem. Soc. 112 (1990) 8251–8260.
[29] E. Cances, B. Mennucci, J. Tomasi, J. Chem. Phys. 107 (1997) 3032–3041.
[30] M.V. De Almeida, J.V. de Assis, M.R.C. Couri, C.P.A. Anconi, M.C. Guerreiro, H.F. dos Santos, W.B. De Almeida, Org. Lett. 12 (2010) 5458–5461.
[31] M.V. De Almeida, M.R. Couri, J.V. de Assis, C.P. Anconi, H.F. dos Santos, W.B. De Almeida, Magn. Reson. Chem. 50 (2012) 608–614.
[32] M.J. Frisch, G.W. Trucks, H.B. Schlegel, G.E. Scuseria, M.A. Robb, J.R. Cheeseman, Jr., J.A. Montgomery, T. Vreven, K.N. Kudin, J.C. Burant, J.M. Millam, S.S. Iyengar, J. Tomasi, V. Barone, B. Mennucci, M. Cossi, G. Scalmani, N. Rega, G.A. Petersson, H. Nakatsuji, M. Hada, M. Ehara, K. Toyota, R. Fukuda, J. Hasegawa, M. Ishida, T. Nakajima, Y. Honda, O. Kitao, H. Nakai, M. Klene, X. Li, J.E. Knox, H.P. Hratchian, J.B. Cross, V. Bakken, C. Adamo, J. Jaramillo, R. Gomperts, R.E. Stratmann, O. Yazyev, A.J. Austin, R. Cammi, C. Pomelli, J.W. Ochterski, P.Y. Ayala, K. Morokuma, G.A. Voth, P. Salvador, J.J. Dannenberg, V.G. Zakrzewski, S. Dapprich, A.D. Daniels, M.C. Strain, O. Farkas, D.K. Malick, A.D. Rabuck, K. Raghavachari, J.B. Foresman, J.V. Ortiz, Q. Cui, A.G. Baboul, S. Clifford, J. Cioslowski, B.B. Stefanov, G. Liu, A. Liashenko, P. Piskorz, I. Komaromi, R.L. Martin, D.J. Fox, T. Keith, M.A. Al-Laham, C.Y. Peng, A. Nanayakkara, M. Challacombe, P.M.W. Gill, B. Johnson, W. Chen, M.W. Wong, C. Gonzalez, J.A. Pople, Gaussian 03, Revision D.01, Gaussian Inc., Wallingford CT, 2004.
[33] H.F. Dos Santos, A.M.G. Do Val, A.C. Guimarães, W.B. De Almeida, Quim. Nova 22 (1999) 674–676.
[34] C.B. Vicentini, S. Guccione, L. Giurato, R. Ciaccio, D. Mares, G. Forlani, J. Agric. Food Chem. 53 (2005) 3848–3855.
[35] Y.-H. Zhang, B.-F. Shi, J.-Q. Yu, Angew. Chem. Int. Ed. 48 (2009) 6097–6100.
[36] P. Jütten, W. Schumann, A. Härtl, H.-M. Dahse, U. Gräfe, J. Med. Chem. 50 (2007) 3661–3666.
[37] F.H. Allen, O. Kennard, D.G. Watson, L. Brammer, A.G. Orpen, R. Taylor, J. Chem. Soc. Perkin Trans. 2 (1987) S1–S19.
[38] E.J. Valente, J.F. Fuller, J.D. Ball, Acta Cryst. B54 (1998) 162–173.
[39] G.D. Mendenhall, R.L. Luck, R.K. Bohn, H.J. Castejon, J. Mol. Struct. 645 (2003) 249–258.
[40] M.-X. Sun, X. Li, W.-Y. Liu, K. Xiao, Acta Cryst. E65 (2009) o2146.
[41] Z. Majeed, W.R. McWhinnie, K. Paxton, T.A. Hamor, J. Chem. Soc., Dalton Trans. 23 (1998) 3947–3951.